Strategy of competition between two groups based on an inflexible contrarian opinion model

Qian Li,[1,*] Lidia A. Braunstein,[2,1] Shlomo Havlin,[3] and H. Eugene Stanley[1]

[1]*Department of Physics and Center for Polymer Studies, Boston University, Boston, Massachusetts 02215, USA*

[2]*Instituto de Investigaciones Físicas de Mar del Plata (IFIMAR), Departamento de Física, Facultad de Ciencias Exactas y Naturales, Universidad Nacional de Mar del Plata-CONICET, Funes 3350, 7600 Mar del Plata, Argentina*

[3]*Department of Physics, Bar Ilan University, Ramat Gan, Israel*

(Received 17 August 2011; revised manuscript received 26 October 2011; published 1 December 2011)

We introduce an inflexible contrarian opinion (ICO) model in which a fraction p of inflexible contrarians within a group holds a strong opinion opposite to the opinion held by the rest of the group. At the initial stage, stable clusters of two opinions, A and B, exist. Then we introduce inflexible contrarians which hold a strong B opinion into the opinion A group. Through their interactions, the inflexible contrarians are able to decrease the size of the largest A opinion cluster and even destroy it. We see this kind of method in operation, e.g., when companies send free new products to potential customers in order to convince them to adopt their products and influence others to buy them. We study the ICO model, using two different strategies, on both Erdös-Rényi and scale-free networks. In strategy I, the inflexible contrarians are positioned at random. In strategy II, the inflexible contrarians are chosen to be the highest-degree nodes. We find that for both strategies the size of the largest A cluster decreases to 0 as p increases as in a phase transition. At a critical threshold value, p_c, the system undergoes a second-order phase transition that belongs to the same universality class of mean-field percolation. We find that even for an Erdös-Rényi type model, where the degrees of the nodes are not so distinct, strategy II is significantly more effective in reducing the size of the largest A opinion cluster and, at very small values of p, the largest A opinion cluster is destroyed.

DOI: 10.1103/PhysRevE.84.066101 PACS number(s): 89.75.Hc, 89.65.−s, 64.60.−i, 89.75.Da

I. INTRODUCTION

Competition between two groups or among a larger number of groups is ubiquitous in business and politics: the decades-long battle between the Mac and the PC in the computer industry, between Procter & Gamble and Unilever in the personal products industry, among all major international and local banks in the financial market, and among politicians and interest groups in the world of governance. All competitors want to increase the number of their supporters and thus increase their chances of success. In gathering supporters, competitors put much effort into persuading skeptics and those opponents who may actually be potential supporters. This kind of activity is normally modeled as a dynamic process on a complex network in which the nodes are the agents and the links are the interactions between agents. The goal of these models is to understand how an initially disordered configuration can become an ordered configuration through the interaction between agents. In the context of social science, order means agreement and disorder means disagreement [1,2]. Most of these models—e.g., the Sznajd model [3], the voter model [4,5], the majority rule model [6,7], and the social impact model [8,9]—are based on two-state spin systems which tend to reduce the variability of the initial state and lead to a consensus state in which all the agents share the same opinion. However this consensus state is not very realistic, since in many real competitions there are always at least two groups that coexist at the same time.

Recently a nonconsensus opinion (NCO) model [10] was developed, where two opinions A and B compete and reach a nonconsensus stable state. At each time step each node adopts the opinion of the majority in its "neighborhood," which consists of its nearest neighbors and itself. When there is a tie, the node does not change its state. Considering also the node's own opinion leads to the nonconsensus state. The dynamics are such that a steady state in which opinions A and B coexist is quickly reached. It was conjectured, and supported by intensive simulations [10], that the NCO model in complex networks belongs to the same universality class as percolation [10–12].

The concepts of inflexible agents and contrarian agents were introduced by Galam *et al.* in their recent work on opinion models [13–16]. However, till now, no one has explored the opinion model with "inflexible contrarians." Here we test how competition strategies are affected when "inflexible contrarians" are introduced. Inflexible contrarians are agents who hold a strong opinion that is opposite to the opinion held by the rest of the group [13,14]. And the inflexible here means that once the contrarians are chosen, they will not change their opinions under any circumstances [15,16]. We develop a spin-type inflexible contrarian opinion (ICO) model in which inflexible contrarian agents are introduced into the steady state of the NCO model. The goal of the inflexible contrarians is to change the opinions of the current supporters of the rival group [17]. We see this strategy in operation, for example, when companies send free new products to potential customers in order to convince them to adopt the products and encourage their friends to do the same. We can observe it also in political campaigns when candidates "bribe" voters by offering favors. The questions we ask in our model are as follows. Do these free products and bribes work and how? Who are the best individuals to chose as inflexible contrarians in order to make the most impact on opinion change.

*liqian@bu.edu

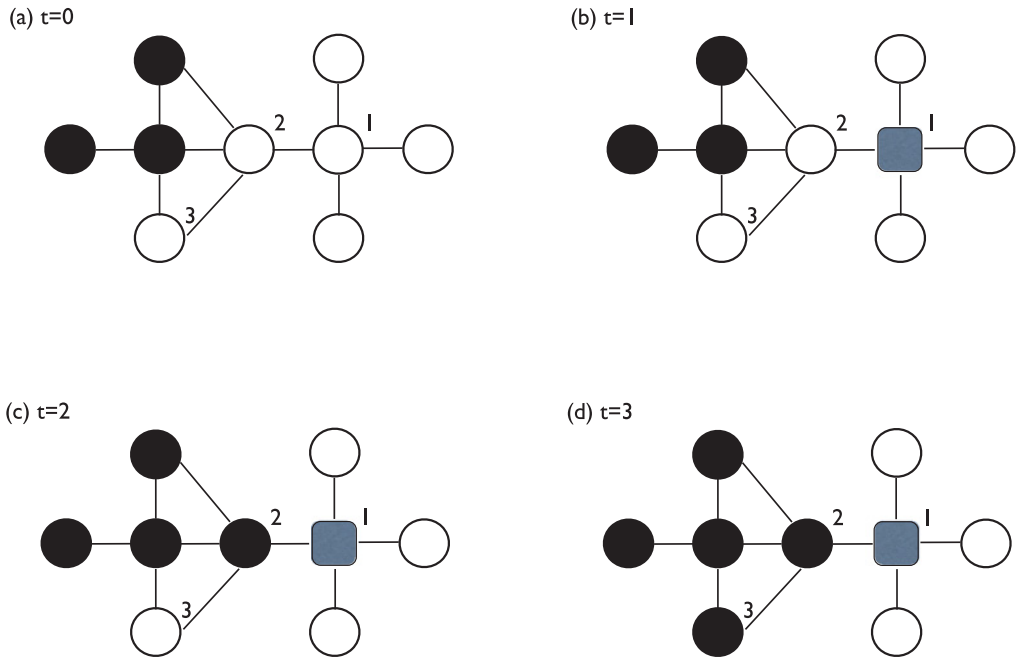

FIG. 1. (Color online) Schematic plot of the dynamics of the ICO model showing the approach to a stable state on a network with $N = 9$ nodes. (a) At $t = 0$, we have a stable state where opinion A (open circle) and opinion B (solid circle) coexist. (b) At $t = 1$, we change node 1 into an inflexible contrarian (solid square), which will hold B opinion. Node 2 is now in the local minority opinion while the remaining nodes are not. Notice that node 1 is an inflexible contrarian and even if he (she) is in the local minority he (she) does not change his (her) opinion. At the end of this simulation step, node 2 is converted into B opinion. (c) At $t = 2$, node 3 is in the local minority opinion and therefore will be converted into B opinion. (d) At $t = 3$, the system reaches a stable state where the system breaks into four disconnected clusters, one of them composed of six B nodes and the other three with one A node.

In this paper we introduce, into group A, a fraction p of inflexible contrarians, which are defined to be agents that hold a strong B opinion, who will influence those who hold the A opinion to change their opinion to B. We study two different strategies of introducing inflexible contrarians: (I) random choosing of inflexible contrarians and (II) targeted. We study these strategies on two types of networks: Erdös-Rényi (ER) [18,19] and scale free (SF) [20,21]. We find, for both strategies, that the relative size of the largest cluster in state A undergoes a second-order phase transition at a critical fraction of inflexible contrarians p_c. Moreover we find that, for both networks analyzed here, the targeted strategy is much more efficient than the random strategy. Our results indicate that the observed second-order phase transition can be mapped into mean-field percolation.

II. THE ICO MODEL

In the NCO model [10], initially, a fraction f of agents with A opinions and $1 - f$ with B opinions are selected at random. At each time step, each network node adopts the majority opinion based on the opinions of its neighbors and itself. All updates are performed simultaneously at each time step until a steady state is reached in which both opinions coexist, which occurs for f above a critical threshold $f \equiv f_c$.

In our ICO model, the initial state is the final state of the NCO model. Above f_c we have stable clusters of both A or B opinions in a network of N agents. We choose, initially, a fraction p of A opinion agents that are changed into B opinion agents and so become inflexible contrarians. By inflexible contrarian we mean that they will never change their opinion but they can influence others. Then we use again the NCO dynamics to reach a new steady state. In the new steady state the agents form again clusters of two opposite opinions above a certain threshold f_c that now depends on p. Because of the inflexible contrarians of type B, the A clusters become smaller and the B clusters increase. In Fig. 1 we show a schematic plot of the dynamics of the ICO model.

We use both random and targeted strategies to choose a fraction p of A agents that flip into state B, and we analyze the results on ER and SF networks. In strategy I we randomly choose a fraction p of A agents, and in strategy II we choose the top p percent of the highest-degree A agents, to become inflexible contrarians. Notice that the inflexible contrarians act as a quenched disorder in the network [11,22].

III. SIMULATION RESULTS

We perform simulations of the ICO model in complex networks, on both ER and SF networks. ER networks are characterized by a Poisson degree distribution with $P(k) = e^{-\langle k\rangle}\langle k\rangle^k/k!$, where k is the degree of a node and $\langle k\rangle$ is the average degree [18]. In SF networks the degree distribution is given by $P(k) \sim k^{-\lambda}$, for $k_{\min} \leqslant k \leqslant k_{\max}$, where $k_{\min}$ is the smallest degree, $k_{\max}$ is the degree cutoff, and λ is the exponent characterizing the broadness of the distribution [20]. In all our simulations we use the natural cutoff, which is controlled

by $N^{1/(\lambda-1)}$ [23]. We performed all the simulations for 10^3 network realizations.

A. ICO model on ER networks

We denote by S_1 the size of the largest A cluster in the steady state. We study the effect of the inflexible contrarians. In Fig. 2 we plot $s_1 \equiv S_1/N$ as a function of f for different values of p for ER networks under both random and targeted strategies. The plot shows that there exists a critical value $f \equiv f_c$ that depends on p, below which s_1 approaches 0. As p increases, the largest cluster becomes significantly smaller as well as less robust, as can been seen from the shift of f_c to the larger value. In the inset of Fig. 2, we plot the size of the second largest A cluster, S_2, as a function of f for different values of p. S_2 shows a sharp peak characteristic of a second-order phase transition, where s_1 is the order parameter and f is the control parameter. Above a certain value of $p \equiv p^*$, the phase transition does not occur because, above p^*, the average connectivity of the A nodes decreases dramatically, the networks break into small clusters, and no giant component of opinion A appears. In Fig. 3 we show, for both strategies, the average degree $\langle k \rangle$ of the A opinion agents as a function of f for different values of p. As shown in Ref. [10] for $p = 0$, $\langle k \rangle$ has a significant increase above $f = 0.5$ where the nodes with opinion A are the majority. This is because when these nodes are in the minority group, they have a small average connectivity since the minority group does not include high-degree nodes [10]. This process is analogous to targeted removing of the high-degree nodes. Only when they become majority nodes, close to $f = 1$, is the original connectivity of the full network recovered. However, as p increases, we never reach the original average degree of the full network because increasing p is equivalent to increasing the quenched disorder. It is known that for ER networks the transition is lost when $\langle k \rangle < 1$ [18]. As we can see from the plots, for $p^* \approx 0.6$ (strategy I) and $p^* \approx 0.4$ (strategy II), $\langle k \rangle$ drops below 1, and then the giant component cannot be sustained.

The loss of robustness is significantly more pronounced in the targeted strategy compared to the random strategy, as seen in Fig. 2(c), where we plot f_c as a function of p for both strategies. From this plot we can see that the targeted strategy is significantly more efficient to annihilate the opinion A clusters than the random strategy. For example, for $p = 0.2$, the network is 25% less robust in the targeted strategy compared to the random one. The reason is that the initial state of our model is the final state of the NCO model, which above its threshold has clusters of nodes A of all sizes. Thus under the random strategy we select nodes at random that are mainly in small A clusters. Under the targeted strategy the selection of inflexible contrarians from the nodes of the highest degree

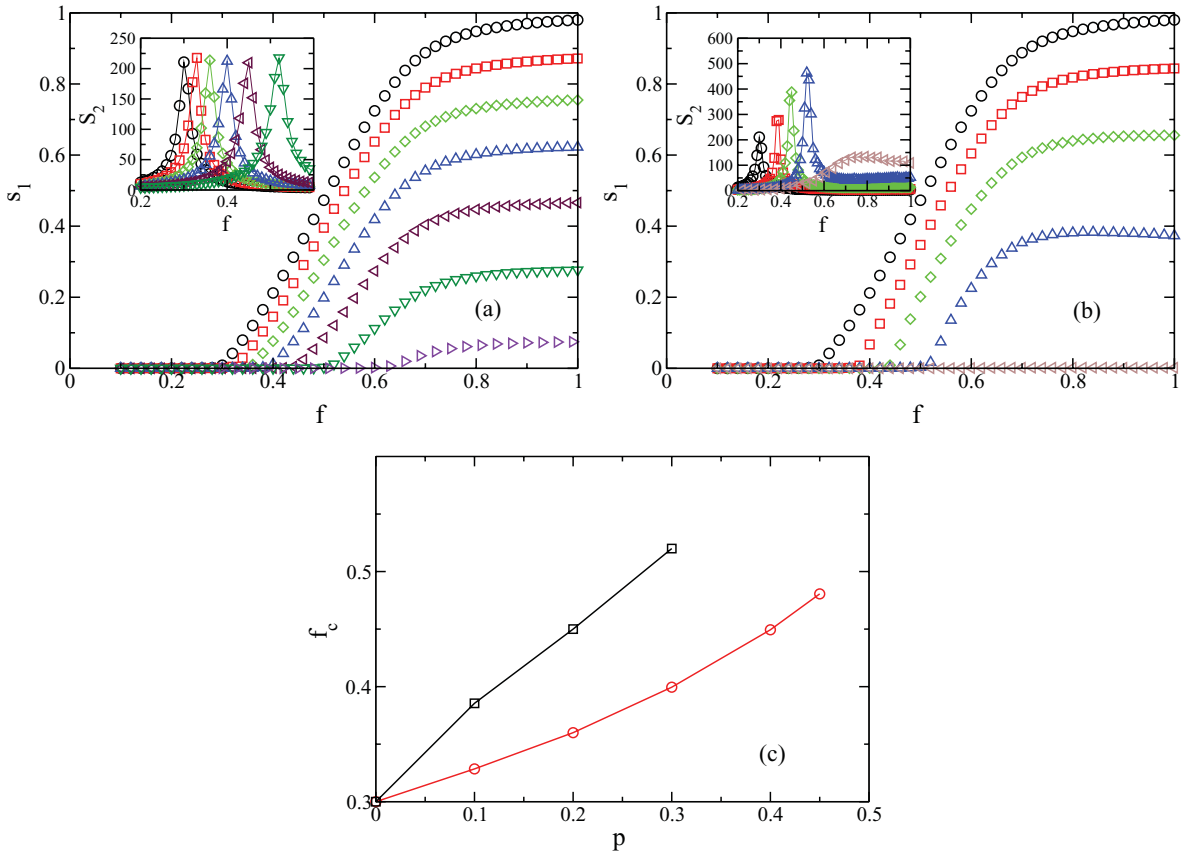

FIG. 2. (Color online) Plot of s_1 as a function of f for different values of p for ER networks with $\langle k \rangle = 4$ and $N = 10^5$. (a) Strategy I: $p = 0$ (○), 0.1 (□), 0.2 (◇), 0.3 (△), 0.4 (◁), and 0.5 (▽) and $p = p^* = 0.6$ (▷). (b) Strategy II: $p = 0$ (○), 0.1 (□), 0.2 (◇), and 0.3 (△) and $p = p^* = 0.4$ (◁). In the inset we plot, using the same symbols as in the main figure, S_2 as a function of f for both strategies. (c) Plot of f_c as a function of p for strategy I (○) and strategy II (□).

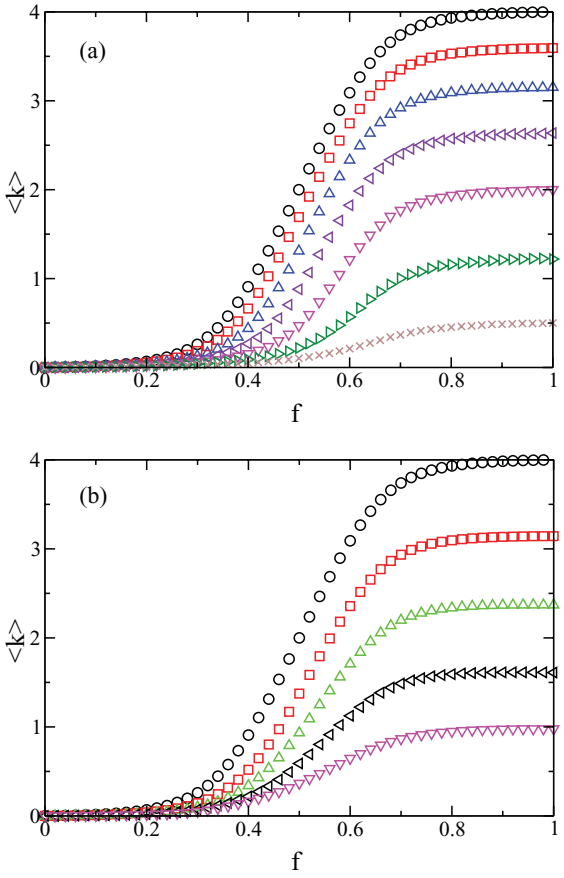

FIG. 3. (Color online) Plot of $\langle k\rangle$ as a function of f for different value of p for ER networks with $\langle k\rangle = 4$ and $N = 10^5$. (a) Strategy I: $p = 0$ (○), 0.1 (□) 0.2 (△), 0.3 (◁), 0.4 (▽), 0.5 (▷), and 0.6 (x). (b) Strategy II: $p = 0$ (○), 0.1 (□) 0.2 (△), 0.3 (◁), and 0.4 (▽).

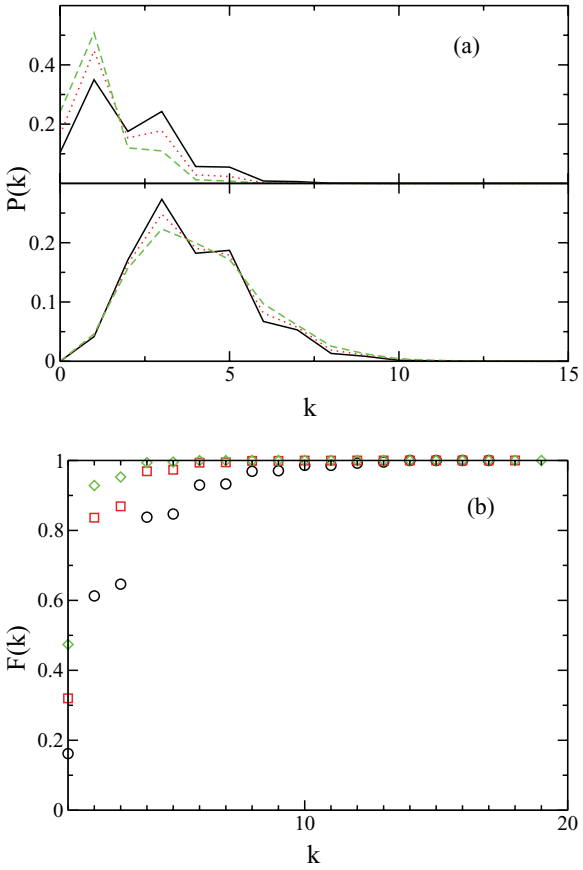

FIG. 4. (Color online) For ER network with $\langle k\rangle = 4$ and $N = 10^5$. (a) Degree distribution $P(k)$ of A nodes as a function of k in our initial configuration with different values of f: $f = 0.35$ (solid line), $f = 0.4$ (dotted line), and $f = 0.45$ (dashed line). In the top panel, we show $P(k)$ as a function of k of the finite A clusters, and in the bottom panel we show the same for the largest A cluster. (b) Plot of $F(k)$ as a function of k for different values of f: $f = 0.35$ (○), 0.4 (□), and 0.45 (◇).

places them mainly in the largest initial A cluster where they can have more influence than if they were isolated in smaller clusters, as in the random strategy. The high-degree nodes shorten the distances between all the pairs of nodes in a cluster, which allows them to interact more easily. Also, because they have many neighbors, they can influence the opinions of other A nodes more efficiently.

In order to verify the above arguments, we compute, for our initial condition ($p = 0$) before adding the inflexible contrarians, the degree distribution of nodes A inside and outside the largest cluster. In Fig. 4(a) we plot the degree distributions $P(k)$ of A nodes inside and outside the largest cluster for three different values of f above the threshold of the NCO model. Notice that the nodes outside the largest cluster have a degree distribution with a high probability of low connectivity. The probability of low connectivity increases as f increases, and thus under a targeted strategy the nodes in those small clusters are almost never designated as inflexible contrarians. Thus nodes in the largest component are more likely to be selected under a targeted strategy than under a random one.

In order to further test our assumption, we compute the fraction $F(k)$, defined as the ratio of the number of nodes with degree k in the largest A cluster and the total number of nodes in all the A clusters with the same degree. When $F(k) \to 1$, all the nodes with degree k are in the largest A cluster. In Fig. 4(b), we plot $F(k)$ as a function of k for different values of f. As k increases, we see that $F(k) \to 1$ is faster for increasing f because the larger f is the larger S_1 will be. Thus the highest-degree nodes belong to the largest cluster and the lower-degree nodes are less likely to be in the largest cluster. This explains why a targeted strategy is significantly more efficient than a random one.

Because p is our main parameter, we next investigate the behavior of the system as a function of p for different values of f. In Fig. 5 we plot s_1 as a function of p for fixed f for ER networks under both strategies. From the plot we can see that S_1 is more robust as f is larger, and the behavior of the curve is again characteristic of a second-order phase transition. However this curve seems to be smoother than the transition found above (see Fig. 2) with f as the control parameter.

In the inset of Fig. 5(a) we plot the first derivative of s_1 with respect to p for two different system sizes for $f = 0.4$. We can see a jump that becomes sharper as the system size increases. We find the same behavior for other values of f

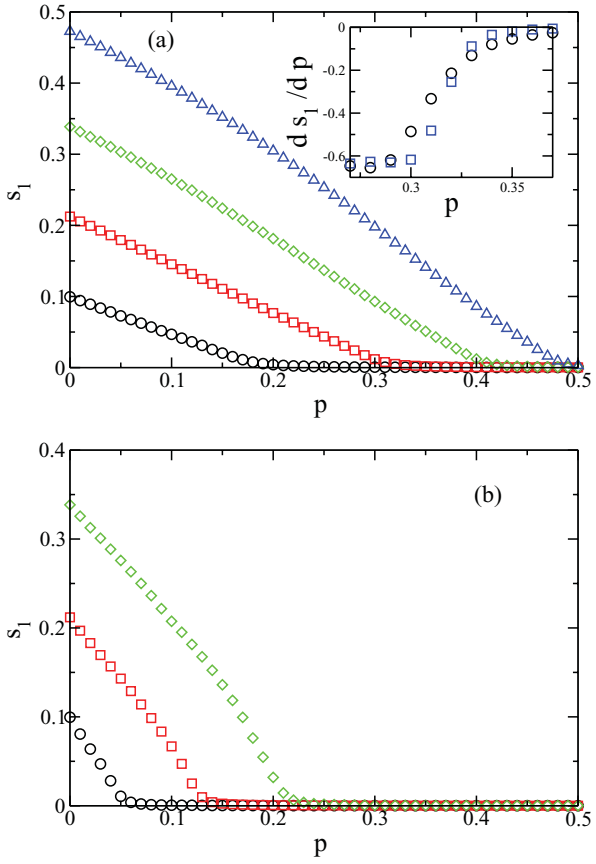

FIG. 5. (Color online) Plot of s_1 as a function of p for different values of f for ER network with $\langle k \rangle = 4$ and $N = 10^5$. (a) Strategy I: $f = 0.35$ (○), 0.4 (□), 0.45 (◇), and 0.5 (△). (b) Strategy II: $f = 0.35$ (○), 0.4 (□), and 0.45 (◇). In the inset of panel (a), we plot the first derivative of $s_1 = S_1/N$ with respect to p (ds_1/dp) with different system sizes: $N = 10^5$ (○) and $N = 10^6$ (□).

above the threshold. In Figs. 6(a) and 6(b) we show S_2 and the first derivative of s_1 with respect to p for $N = 10^5$ and for different values of f. We find that the peak of S_2 and the jump of the derivative of s_1 occurs at the same value of p. This behavior is characteristic of a second-order phase transition, where the peak of S_2 indicates the position of the threshold p_c. In Fig. 6(c) we plot the critical threshold p_c as a function of f for both strategies. Comparing the two strategies for the same value of f, strategy II always has the smaller p_c. This demonstrates again that strategy II is better because a very small fraction of p is enough to destroy the A opinion clusters.

Next, we present results indicating that the ICO model is in the same universality class as regular percolation. Percolation in random networks (e.g, ER) [11,12,21] predicts that at criticality the cluster size distribution of finite clusters $n_s \sim s^{-\tau}$ with $\tau = 2.5$. In Fig. 7 we plot n_s for both random and targeted strategies as a function of s for finite A clusters at criticality. As we can see for both strategies, $\tau \approx 2.5$. Moreover, from S_2 we calculate the exponent γ, which represents how the mean finite size diverges with distance to criticality (not shown here), from which we obtain $\gamma \approx 1$, as in mean-field percolation. The values of the two exponents we obtain strongly indicate that our ICO model in ER networks is in the same universality class as mean-field percolation in complex networks below p^* [24].

B. ICO model on SF networks

Many real social networks are not ER, but instead possess a SF degree distribution. It is well known that dynamic processes in SF networks propagate significantly more efficiently [25–30] than in ER networks. For SF networks we find that the system also undergoes a second-order phase transition as in ER networks with mean-field exponents (not shown here).

In Fig. 8(a) we plot f_c as a function of p for SF networks with $\lambda = 3.5$. For a certain value of p, when $f < f_c$, we lose the largest A cluster. Thus the larger the value of f_c the less robust the networks are. From the plot, we find that for all values of p, strategy II has much larger f_c than strategy I. This shows that SF networks are significantly less robust under strategy II than under strategy I, which shows that, for SF networks, strategy II is significantly more efficient compared to strategy I. To further test our conclusion, in Fig. 8(b), we plot p_c as a function of f for the same SF networks. As p_c is the minimum concentration of inflexible contrarians needed to destroy the largest A cluster, for the same initial condition, the networks are less robust with smaller p_c than with larger p_c. As shown in Fig. 8(b), for the same value of f, p_c under strategy II is always significantly smaller than that under strategy I. This result again supports our former conclusion that, for SF networks, strategy II is more efficient than strategy I. As mentioned above, this is because the targeted strategy sends most of the inflexible contrarians into the largest A cluster. In order to test that, in Fig. 9 we plot $F(k)$ as a function of k for SF networks. As we can see from Fig. 9, almost all of the high-degree nodes ($k \gtrsim 10$) belong to the largest A cluster. This behavior is more pronounced as f increases because S_1 increases with f.

C. Comparison between ER and SF networks

If we compare all our results between ER and SF networks, we find that both strategies are more efficient for SF networks. For example, when we compare Fig. 8(a) with Fig. 2(c) we see that for all the values of p, f_c for SF networks is larger than that for ER networks for both strategies. The main difference between ER and SF networks is that SF networks possess larger hubs than ER networks, and thus it is more efficient to destroy the largest A cluster. We also find that the targeted strategy is more efficient in SF networks than in ER networks due to the presence of these large hubs. For example, when $p = 0.1$, the SF network is 64% less robust under the targeted strategy than under the random strategy. In ER networks, for the same value of p, the robustness of the networks decreases only by 17%. If we compare Fig. 4(b) with Fig. 9 we see that higher degree nodes are more likely to belong to the largest cluster in SF networks than in ER networks, since $F(k) \to 1$ faster in SF networks compared to ER networks.

D. Minority vs majority

When two groups compete, either group can use both random and targeted strategies to influence the other group. Will the impact of these strategies differ if the group using

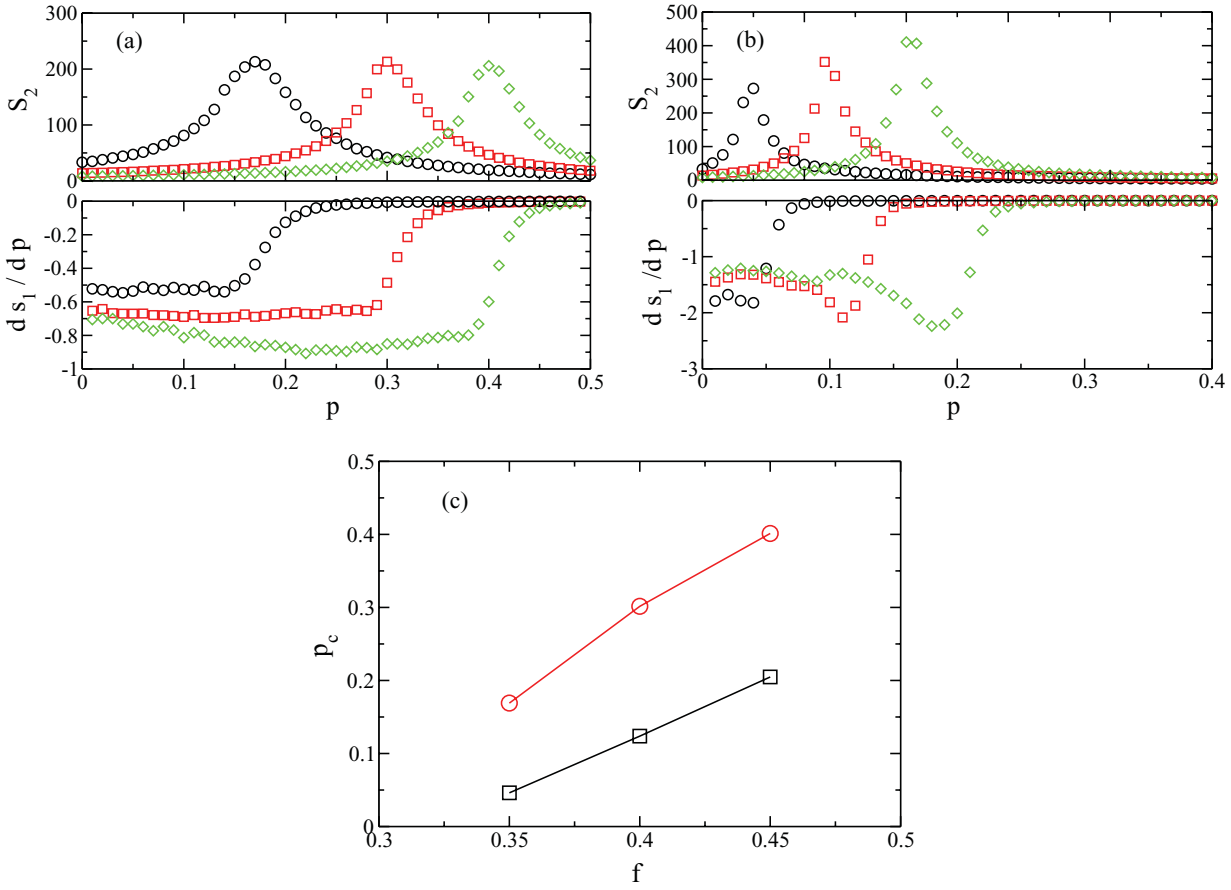

FIG. 6. (Color online) Plot of S_2 as a function of p (top panel) and ds_1/dp as a function of p (bottom panel) for different values of f for (a) strategy I and (b) strategy II [$f = 0.35$ (○), 0.4 (□), 0.45 (◇)] for ER networks with $\langle k \rangle = 4$ and $N = 10^5$. We can see that in both cases the peak of S_2 coincides with the position of the jump, also indicating a second-order phase transition. In panel (c) we plot p_c as a function of f for both strategies: strategy I (○) and strategy II (□).

them is in the majority, as opposed to being in the minority? Because the largest majority cluster will have a larger average degree than the largest minority cluster, we assume it will be harder to change the opinion of the majority than the minority for $p < p_c$. In order to quantitatively understand the effect of inflexible contrarians in both a minority group and a majority group, we compute the relative change of the size of the largest minority and majority clusters, ΔS_1, given by

$$\Delta S_1 = \left(S_1^{\text{initial}} - S_1^{\text{final}}\right)/S_1^{\text{initial}},$$

where S_1^{final} is the size of the largest A cluster in our final steady state and S_1^{initial} is the cluster before adding the inflexible contrarians. Notice that $f < 0.5$ ($f > 0.5$) means that the A agents are minority (majority). We compute ΔS_1 for $f = 0.55$ (majority) to compare with $f = 0.45$ (minority). For a more extreme case like $f = 0.8$ (majority) and $f = 0.2$ (minority), as can be seen in Fig. 3, when $f = 0.2$, the average degree of minority agents is close to 0. This means that there exist only small minority clusters and the influence of inflexible contrarians is negligible since one can change the minority opinion of an agent mostly when one becomes an inflexible contrarian oneself. We therefore focus on intermediate f values, where our results show that, even when the size of the majority group and the size of the minority group are very close (one is slightly bigger than the other), still the power of the inflexible contrarians placed in the minority is significantly higher than that of the inflexible contrarians placed in the majority. In Fig. 10 we plot ΔS_1 as a function of p for $f = 0.45$

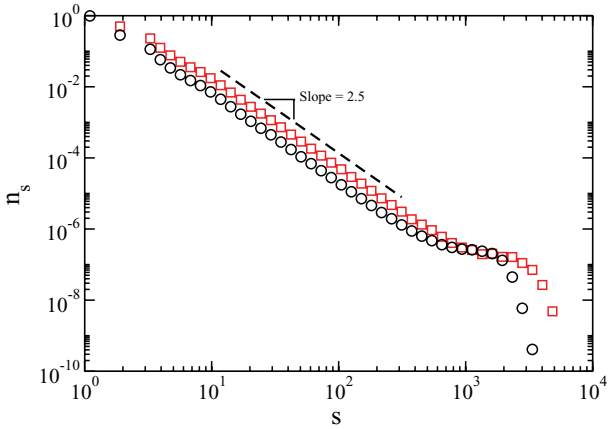

FIG. 7. (Color online) Plot of n_s as a function of s under strategy I (○) and strategy II (□) for ER networks with $\langle k \rangle = 4$ and $N = 10^5$ at criticality $p = p_c$. The dashed line represents a slope $\tau = 2.5$. These simulations were done over 10^5 realizations.

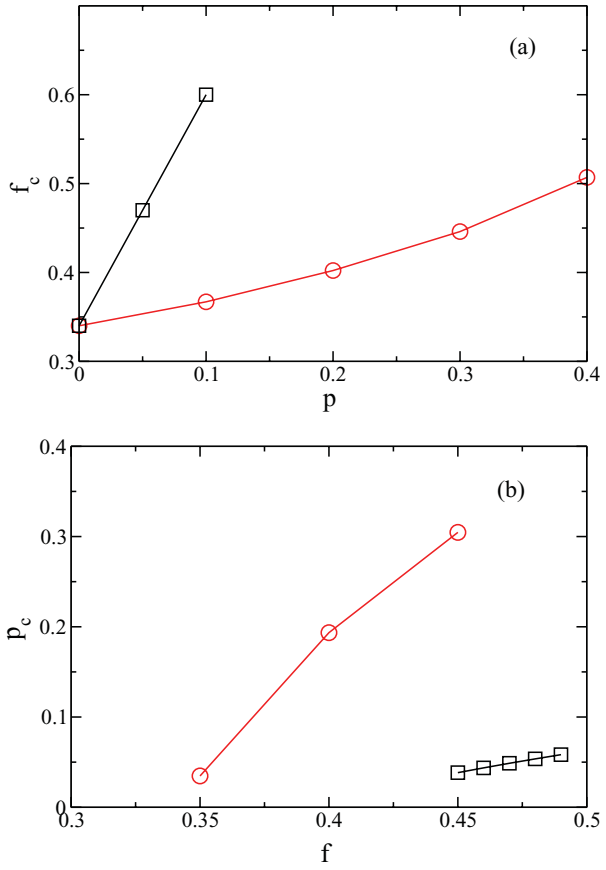

FIG. 8. (Color online) Plot of (a) f_c as a function of p and (b) p_c as a function of f for strategy I (○) and strategy II (□) for SF networks with $\lambda = 3.5$, $k_{\min} = 2$, and $N = 10^5$.

(minority) and $f = 0.55$ (majority) under both strategies for both ER and SF networks. From the plots we can see that below p_c (marked by arrows in the plots), ΔS_1 is larger for the minority than for the majority for the same value of p, under both strategies I and II, and for the two networks used

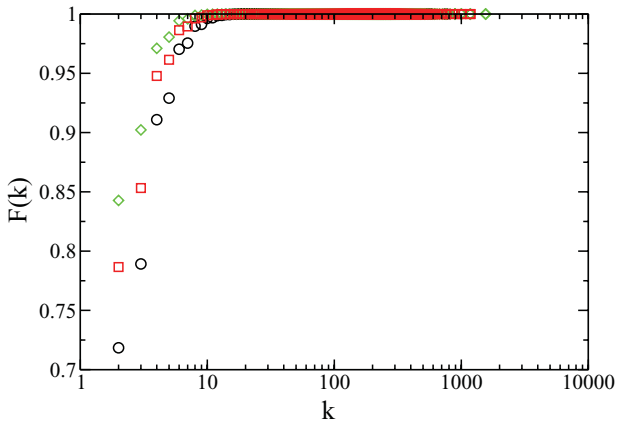

FIG. 9. (Color online) Plot of $F(k)$ as a function, in linear-log scale, of k for ER networks with $\langle k \rangle = 4$ and $N = 10^5$ with different values of f: $f = 0.35$ (○), 0.4 (□), 0.45 (◇). The reason for using linear-log scale is that for SF networks $F(k)$ increases very fast for small values of k.

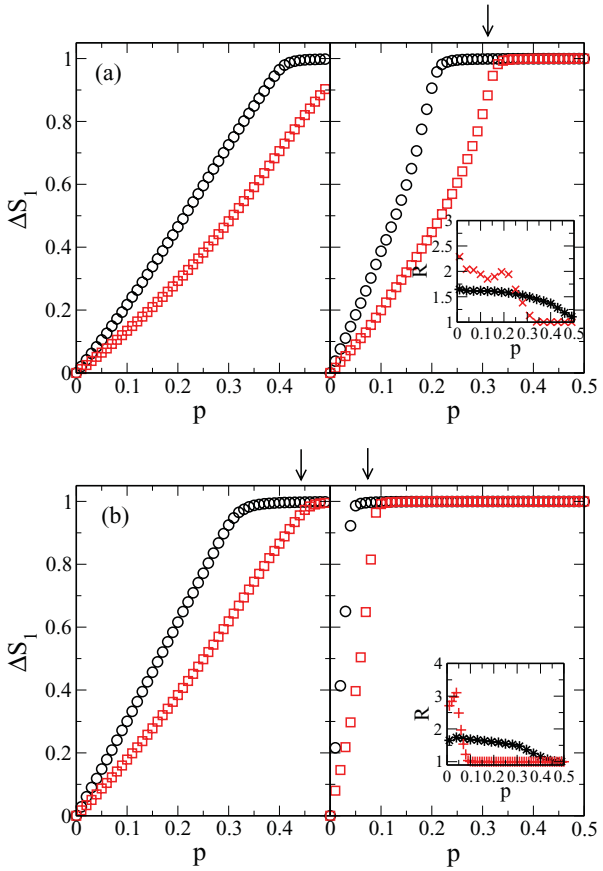

FIG. 10. (Color online) Plot of ΔS_1 as a function of p for $f = 0.45$ (○) and for $f = 0.55$ (□) under strategy I (left plot) and strategy II (right plot) for (a) ER networks with $\langle k \rangle = 4$ and $N = 10^5$ and (b) SF networks with $\lambda = 3.5$ and $N = 10^5$. The arrows indicate the position of p^* above which there is no phase transition. In the insets we show the ratio R between ΔS_1 for $f = 0.45$ and ΔS_1 for $f = 0.55$ for strategy I (∗) and strategy II (x). All the simulations were done for 10^5 network realizations.

here, ER and SF. Thus, as argued above, the minority groups are easier to convince than the majority groups. Moreover, this phenomenon is more pronounced under the targeted strategy than under the random strategy. In the inset of Fig. 10 we plot R, which is the ratio between ΔS_1 of the minority and ΔS_1 of the majority, as a function of p. As we can see for the ER network, the inflexible contrarians under a targeted strategy are twice as effective when they are in the minority group than when they are in the majority group, while under a random strategy they are approximately 1.5 times more effective. We can see a similar but more significant tendency in SF networks. This agrees with empirical fact, where majority groups always have more power than minority groups, and thus it is easier for a majority group to change the opinion of a minority group. We conclude that our model seems to mimic well the two-group competition in the real world and that it also reveals some underlying complex phenomena associated with the process.

IV. CONCLUSIONS

In introducing inflexible contrarians into a system, we have used two strategies: (i) random and (ii) targeted. Our inflexible

contrarians hold a strong B opinion and the system has two stable opinion A clusters and opinion B clusters. We find that, for both strategies, the size of the largest A opinion cluster shrinks, as in a phase transition phenomena. As the concentration of inflexible contrarians increases, the largest A cluster becomes smaller and smaller until it reaches 0 at a critical concentration p_c. Above p_c, the largest A cluster disappears. Our results show that the system undergoes a second-order phase transition for both control parameters f and p, behavior that resembles mean-field percolation. We also find that, for both ER and SF networks, the targeted strategy is more efficient than the random strategy because the targeted strategy always sends more inflexible contrarians into the largest cluster than the random strategy. Both strategies affect more the minority group and much less the majority group. Note that since SF networks have hubs, both strategies work better in SF networks than in ER networks. Based on our results, we can answer the questions we raise in the Introduction. Free products and favors ("bribes") do effectively attract more supporters, but the most effective strategy is to target those potential supporters with the most connections and offer the free products and favors to them. We also note that our ICO results support Galam's conclusion that inflexible agents do play a key role in winning a public debate [31], as in our ICO model inflexible contrarians play a key role in changing others' group opinion.

ACKNOWLEDGMENTS

We thank Jia Shao for discussions, and UNMdP, FONCYT-PICT 2008/0293, ONR, DTRA, DFG, EU Project Epiwork, and the Israel Science Foundation for financial support.

[1] C. Castellano, S. Fortunato, and V. Loreto, Rev. Mod. Phys. **81**, 591 (2009).
[2] S. Galam, Europhys. Lett. **70**, 705 (2005).
[3] K. Sznajd-Weron and J. Sznajd, Int. J. Mod. Phys. C **11**, 1157 (2000).
[4] T. M. Liggett, *Stochastic Interacting Systems: Contact Voter, and Exclusion Processes* (Springer, Berlin, 1999).
[5] R. Lambiotte and S. Redner, Europhys. Lett. **82**, 18007 (2008).
[6] S. Galam, Eur. Phys. J. B **25**, 403 (2002).
[7] P. L. Krapivsky and S. Redner, Phys. Rev. Lett. **90**, 238701 (2003).
[8] B. Latané, Am. Psychol. **36**, 343 (1981).
[9] A. Nowak *et al.*, Psychol. Rev. **97**, 362 (1990).
[10] J. Shao, S. Havlin, and H. E. Stanley, Phys. Rev. Lett. **103**, 018701 (2009).
[11] A. Bunde and S. Havlin, *Fractals and Disordered Systems* (Springer-Verlag, Berlin/New York, 1994).
[12] D. Stauffer and A. Aharony, *Introduction to Percolation Theory* (Taylor & Francis, London, 2003).
[13] S. Galam, Physica A **333**, 453 (2004).
[14] C. Borghesi and S. Galam, Phys. Rev. Lett. **066118**, 1 (2006).
[15] S. Galam, Physica A **238**, 66 (1997).
[16] S. Galam and F. Jacobs, Physica A **381**, 366 (2007).
[17] S. Galam, e-print arXiv:0803.2453.
[18] P. Erdös and A. Rényi, Publ. Math. Inst. Hung. Acad. Sci. **5**, 17 (1960).
[19] A.-L. Barabási, *Random Graphs* (Cambridge University Press, Cambridge, UK, 2001).
[20] A.-L. Barabási and R. Albert, Science **286**, 509 (1999).
[21] R. Cohen and S. Havlin, *Complex Network: Structure, Robustness and Function* (Cambridge University Press, Cambridge, UK, 2010).
[22] A.-L. Barabási and H. E. Stanley, *Fractal Concepts in Surface Growth* (Cambridge University Press, Cambridge, UK, 1995).
[23] R. Cohen, K. Erez, D. ben-Avraham, and S. Havlin, Phys. Rev. Lett. **85**, 4626 (2000).
[24] In simulations of the NCO model on 2D lattices, Shao *et al.* [10] suggested that it is in the same universality class as invasion percolation. We expect that our ICO model on 2D lattices will be also in the same class as invasion percolation.
[25] R. Pastor-Satorras and A. Vespignani, Phys. Rev. Lett. **86**, 3200 (2001).
[26] E. López, S. V. Buldyrev, S. Havlin, and H. E. Stanley, Phys. Rev. Lett. **94**, 248701 (2005).
[27] Z. Wu, E. Lopez, S. V. Buldyrev, L. A. Braunstein, S. Havlin, and H. E. Stanley, Phys. Rev. E **71**, 045101(R) (2005).
[28] A. E. Motter, Phys. Rev. Lett. **93**, 098701 (2004).
[29] G. Korniss, Phys. Rev. E **75**, 051121 (2007).
[30] M. Boguñá and D. Krioukov, Phys. Rev. Lett. **102**, 058701 (2009).
[31] S. Galam, Physica A **389**, 3619 (2010).